Study on the Impact of Non-Metallic Material Vacuum Volatiles on the Electrical Transmission Performance of Conductive Slip Rings

Zemin Hu, Yijian Wang, Bin Lv, Zengwei Zhou, Hongming Ni, Fei Gao, Peng Luo
CSSC Jiujiang Jingda Technology Co., Ltd, Jiujiang 332000, Jiangxi, China
Corresponding author: Zengwei Zhou (e-mail: LeonChang0226@163.com)

ABSTRACT
Conductive slip rings transmit electrical signals and power through rotational friction, during which wear debris is gradually generated and accumulated. Under vacuum conditions, condensable volatiles released from non-metallic materials may adhere to the friction pair surfaces, affecting contact stability and degrading electromagnetic signal transmission reliability. To investigate the electrical signal dynamic resistance anomalies observed during high- and lowtemperature vacuum tests of column-type slip rings in spacecraft drive mechanisms, experiments were conducted to evaluate the influence of condensable organic volatiles on the electrical transmission performance of conductive slip rings in a vacuum environment. The results show that non-metallic materials release volatile substances under vacuum conditions, with elemental analysis identifying C, O, Si, S, and Cl as the primary non-metallic components. Spectral analysis of the organic materials and comparative characterization indicate that GD-414C adhesive is the major source of the condensed organic mixture. The accumulation of these volatiles on slip ring friction pair surfaces promotes wear debris aggregation and leads to significant electrical signal dynamic resistance anomalies. The findings provide theoretical support for contamination control and electromagnetic transmission reliability enhancement in high-reliability rotary electrical interfaces operating in vacuum environments.

INDEX TERMS
conductive slip ring, vacuum volatiles, electromagnetic signal transmission, dynamic contact resistance, contamination control

I. INTRODUCTION

THE space-grade slip ring, as a core component of the spacecraft's rotary electrical transmission system, facilitates the transfer of power and signals between relatively rotating mechanisms through the sliding action of brushes on the ring path, playing a crucial role in various space rotation devices[1]. As a space operational component that requires long-term in-orbit operation, its safety, reliability, and operational lifespan are directly linked to the success or failure of the spacecraft's in-orbit missions, making it one of the few single-point failure devices on various spacecraft [2]. The figure below (Figure 1) shows the specific mechanical structure of a certain model of space-grade slip ring.

With the increasing demand of modern space missions for high-power, long-life space rotary mechanisms, power-type slip rings have seen their reliability become a key concern in satellite system engineering, requiring durability standards comparable to the high-frequency rotary components utilized in continuous-operation machinery[3-5]. Research by Wang et al.[3] indicates that momentary interruptions are the primary performance indicator of precision slip rings and can lead to attitude jump faults. Studies by Argibay et al.[4] and colleagues show that in the absence of current, the wear mechanism is mainly abrasive wear, which gradually converts to electrical wear as the current increases. Grandin and Wiklund [5] and explored the relationship between electrical contact materials with different Ag contents and the service life of slip rings, aiming to improve the wear resistance and electrical conductivity during relative motion of the contact materials. Bouchoucha et al.[6] and colleagues verified the reliability of a specific type of satellite-mounted columnar slip ring under a requirement of one million rotations in orbit, investigating the transmission reliability of power and signal rings under two different brush structures—single brushes and brush bundles— at the end of the life test. The stability of electrical signal transmission in in-orbit satellite

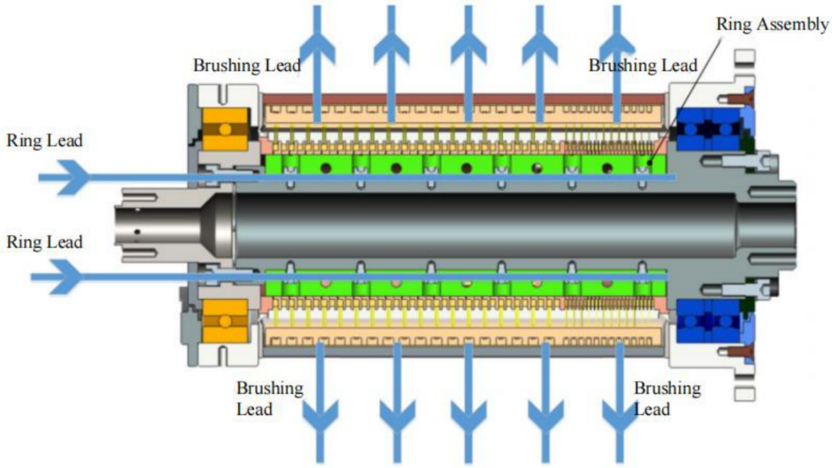

FIGURE 1. Schematic Diagram of the Spatial Conductive Slip Ring Structure

operations is an important indicator of the high reliability of slip rings. During the development of slip rings, non-metallic materials are used, and the condensable substances that evaporate under vacuum conditions and condense on the surface of the slip ring channels significantly affect the stability of electrical signal transmission, thereby reducing the reliability of the slip rings[7]. To select slip ring products with higher reliability, it is usually necessary to conduct vacuum-powered running-in tests and thermal vacuum tests on the ground, using data acquisition instruments to collect the product's voltage drop and electrical noise results as criteria for good electrical transmission stability. Satellites typically require a slip ring service life of 10 years or longer. Due to the high difficulty and cost of maintenance, the products are required to have high reliability[8]. Electrical signal dynamic resistance anomalies indicate reduced satellite reliability and can directly lead to the malfunction of certain spacecraft systems. Therefore, designing and developing highly reliable slip rings holds significant engineering value for enhancing spacecraft in-orbit operation and provides a technical reference for optimizing high-speed rotary transmission in automated equipment.

II. INSTABILITY IN ELECTRICAL TRANSMISSION OF GROUND SLIP RING PRODUCTS

Currently, several models of space conductive slip rings developed by CSSC Jingda Co., Ltd. have exhibited small current electrical signal dynamic resistance anomalies during on-ground vacuum powered operation tests and thermal vacuum tests. Specifically, some of the ring circuits in the conductive slip ring products showed P2P values and electrical noise exceeding technical specification limits during high and low temperature test phases. Since the commencement of vacuum small current testing, a total of 9 units across 5 models have exhibited signal anomalies, as detailed in the table below (Table 1) :

The above experimental results preliminarily indicate that the occurrence of signal anomalies generally happens during the vacuum testing phase. Considering that the conductive slip rings use non-metallic materials such as GD414, HY914, YS20, and 3M tapes during development, the organic compounds they release in a vacuum environment may condense on the surface of the rings, potentially causing signal anomalies. In response to the aforementioned signal anomaly phenomenon, small-current tests and monitoring comparison experiments have been conducted.

TABLE 1. Summary of Small Current Jumps During Vacuum Power-On Break-In of Ground Products

Model	Normal Temperature & Pressure	Vacuum Electrification	Thermal Vacuum Test	Remarks
HJX-K-50DC	None	Jumps occurred in five channels, including A17, A18, A19, and A24	Several jumps occurred in A24 and A27; Excessive multi-channel electrical noise	Vacuum power-on run-in tests and thermal vacuum tests can simulate the vacuum environment and temperatures of space, allowing for maximum reflection of the product's operational status after entering orbit; 2. All the above all transitions occur during the heating and high-temperature maintaining phases.
	None	Jumps occurred in A21 and A29	None	
HJX-K-52DE	None	More than 20 jumps occurred in B03 and B04	None	
HJX-K-60DE	None	More than 10 jumps occurred in B11, A45 and A46	About 10 jumps occurred in A43 and A44	
	None	No transition	Excessive electrical noise occurred in B04	
	None	No transition	Jumps occurred in channels A24, A26, B05, and 12 others during cooling	
HJX-K-70DE		Several jumps occurred in A24 and A25	None	
	None	Several jumps occurred in nine channels including A11, A12, B12, B16, B22 and etc	Not tested	
HJX-K-120M	None	Jumps occurred in a total of 17 test circuits	The jumps are concentrated in the high-temperature stage	

III. TEST IMPLEMENTATION AND PLANNING

(1) Test Subjects

Two aerospace conductive slip rings, A and B, were selected as test products. The ring body is formed by laminated casting, the friction pair is PdNi-Au AuNi9; the ring-brush contact uses a V-groove and brush wire contact method. The above conditions are kept consistent with the operational state of the conductive slip rings in orbit.

Both Product A and Product B are aerospace flight models. Prior to this experiment, both products had undergone a "vacuum environment outgassing" process during their development phase, ensuring their initial state was "clean and uncontaminated." Subsequently, both were placed simultaneously in a contamination environment created by non-metallic materials.

(2) Test Variables

Both Product A and Product B have been contaminated by vacuum volatiles from non-metallic materials. Product A's circuits have been thoroughly wiped clean; for Product B, some circuits are left unwiped, while others are cleaned according to the wiping process. Subsequently, a vacuum high/low temperature small-current running-in test and monitoring are conducted. The specific circuit wiping requirements for Product B are shown in the figure below (Figure 2) :

(3) Test Conditions

Tooling Cables: 1 set of mechanical test tooling, 2 sets of product wiring cables, 2 sets of in-tank power connector cables, 2 sets of out-of-tank power cable connectors, and 2 sets of out-of-tank power cables.

Equipment: 1 mechanical refrigeration vacuum tank, 2 sets of vacuum motors with driving circuit boxes, 1 data acquisition instrument, 4 power supplies, and 3 variable resistance boxes (0–50 KΩ);

(4) Test Procedure

Phase 1: Products A and B begin testing in a vacuum volatile contaminant environment created from non-metallic materials. The products are placed in a vacuum chamber for testing, with small current tests conducted during the high and low temperature holding stages, and the rest of the process is monitored with a 0.1mA small current.

Phase 2: After Phase 1 is completed, Products A and B are disassembled, cleaned, dried, and reassembled according to the test variable requirements to reach a test-ready condition. The products are placed in a vacuum chamber along with the running-in fixtures for high and low temperature vacuum powered tests.

The specific powered running-in test conditions for Phases 1 and 2 are shown in the table below (Table 2) :

The entire vacuum high and low temperature test process is as figure below (Figure 3):

(5) Test Instructions

1 Temperature Control Point Setting: The temperature control points are set on the flange end surface near the side of the slip ring with fewer output lines. Temperature measurement points should also be set and recorded on the flange end surface with more slip ring output lines, on the brush holder, and in the middle area of the dust cover;

2 B-Product Slip Ring Cleaning: Use a lint-free cloth moistened with acetone to wipe each slip ring twice, then use an electric toothbrush to remove any remaining debris.

TABLE 2. Test Conditions for Break-in Operation under Vacuum Environment

S/N	A	B	Remark
1	Temperature Range °C	-50; +60	
2	Temperature Change Rate °C/min	≥1	The high-temperature and low-temperature ends of the first and last cycles should remain for at least 6 hours, while the others for 4 hours.
3	Holding Time h	Start-to-end cycle ≥ 4	
4	Number of Cycles	≥ 4.5 (no less than 5 days)	
5	Vacuum Level Pa	Better than ≤ 1.3e-3 Pa; 1.8 (Rated Current Test)	
6	Rotation Speed °/s	0.6 (0.1mA Low Current Monitoring)	

Note: The rotational speed settings are based on current industry practices for aerospace conductive slip ring vacuum testing, as established by major research institutes (e.g., China Academy of Space Technology-5th Institute, 8th Institute).

After cleaning, inspect the slip rings and brush bristles under a microscope for any residual material;

3 Rotational Speed Requirements: For product testing at rated current, control the rotational speed at 1.8°/s; for low current testing at 0.1 mA, control the rotational speed at 0.6°/s as per the industry testing standard;

4 Non-Metallic Material Contamination Environment: Apply a conformal coating with a thickness of 25 μm to 125 μm conformal coating on the test fixture; affix 3M tape around, and apply unde-gassed GD-414C adhesive to simulate the volatile environment of non-metallic materials under vacuum. These unde-gassed materials represent the initial state of the non-metallic components, which will actively release volatiles under the vacuum high-temperature test conditions, thereby constituting a representative contamination environment;

5 Correspondence Between Slip Ring Channels and Data Acquisition Instrument: A01→Channels 1, 2; A02→Channels 3, 4; and so on. The first connector on the data acquisition instrument is numbered A01–A30, and the second connector is numbered B01–B30.

IV. ANALYSIS OF EXPERIMENTAL RESULTS

(1) Analysis of Product A under vacuum at high and low temperatures

The test product A, under high and low vacuum temperature conditions, showed a maximum measured P2P voltage drop of the power ring not exceeding 6.5V, a maximum measured P2P voltage drop of the signal ring not exceeding 3V, and a maximum measured signal ring electrical noise not exceeding 2mV/A, all within the technical specification requirements for conductive slip ring products. The voltage drop and electrical noise curves throughout the full process of 4.5 high and low temperature cycles showed consistent patterns with no abnormalities. Aside from the test duration, small current monitoring was conducted on the test product,

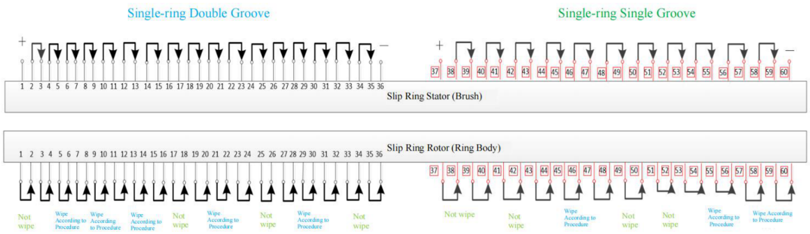

FIGURE 2. Schematic Diagram of Annular Wiping of Test Products

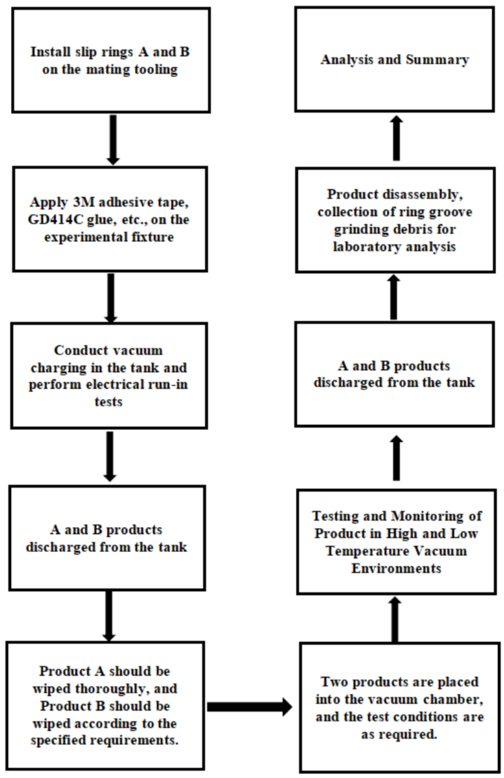

FIGURE 3. Schematic Diagram of the Slip Ring Product Testing Process

and the monitoring results showed no sudden changes, remaining normal. The specific test data are as figures below (Figure 4, Figure 5 and Figure 6):

(2) Analysis of Product B under vacuum at high and low temperatures

During tests on Product B under high and low vacuum temperature conditions, the peak P2P voltage drop measured for the power loop under small current reached 10.0 V, while the peak P2P voltage drop for the signal loop exceeded 4 V. The maximum measured electrical noise of the signal loop did not exceed 3 mV/A, which surpasses the technical specifications for conductive slip ring products. Throughout 4.5 cycles of high and low temperature testing, the voltage drop and electrical noise curves became irregular, yielding abnormal results. Apart from the testing duration, small current monitoring of the test product showed electrical signal dynamic resistance anomalies in multiple channels such as A01, A09, A12, A13, etc. To clearly demonstrate the correlation between contamination state and signal anomalies, the mapping between unwiped loops and anomalous channels is presented in the following Table 3. The channels exhibiting anomalies correspond almost exclusively to the loops that were not wiped as shown in Figure 2, indicating abnormal dynamic contact resistance of the product. The specific test data are as figures below (Figure 7, Figure 8 and Figure 9):

V. ANALYSIS OF VOLATILE COMPONENTS IN THE RING ROAD

After completing the high and low temperature tests in a vacuum environment, Product A was disassembled and the cover removed for inspection. The results showed that the surface debris in the channels was granular, as shown in Figure 10. Since the low-current tests and monitoring results of Product A under high and low temperature conditions were normal, and the dynamic resistance of each circuit under powered conditions was within the specified technical range, the contamination caused by trace vacuum volatilization of

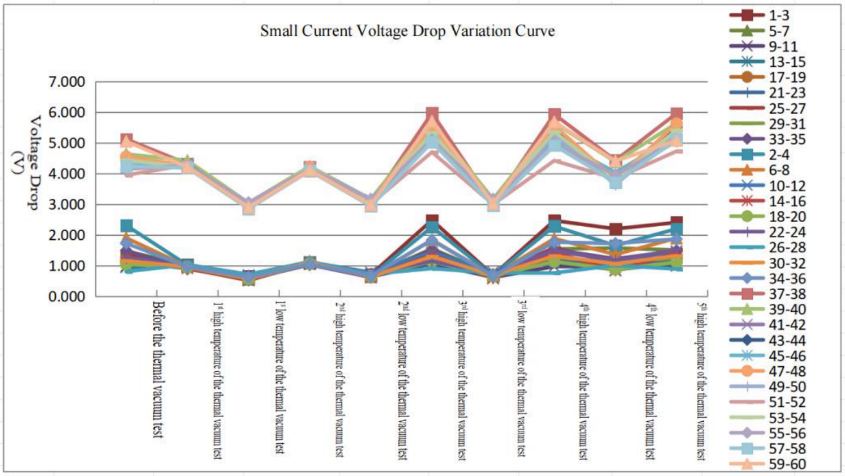

FIGURE 4. P2P Curve of Product A under Vacuum Environment High and Low Temperature Tests

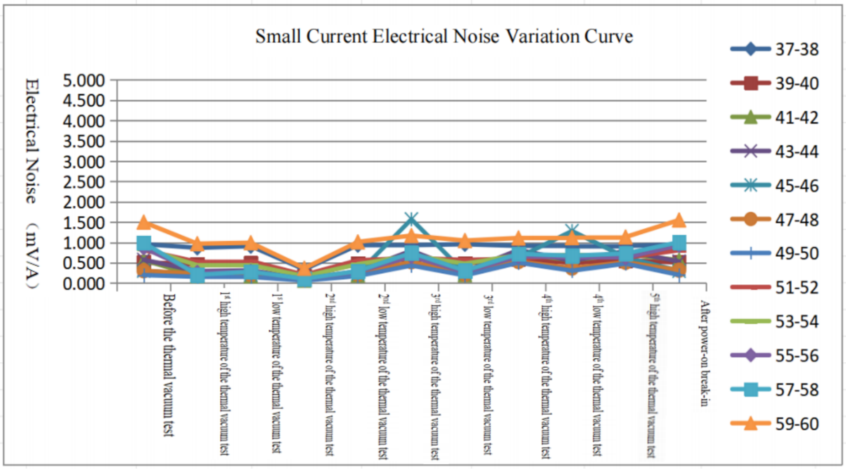

FIGURE 5. Electrical noise diagram of Product A under high and low temperature vacuum conditions

TABLE 3. Correlation Between Loop Wiping Status and Signal Jump Phenomena

Test Product	Loop	Channel	Wiping Status	Signal Jump Phenomenon
Product A	All Loops	A01–A30	Thoroughly wiped clean	Unhappen
Product B	1–4	A01, A02	Not wiped	Happened
	5–8, 9–12, 13–16	A02–A08	Wiped according to procedure	Unhappen
	17–20	A09, A10	Not wiped	Happened
	21–24	A11, A12	Not wiped	Happened
	25–28	A13, A14	Not wiped	Happened
	29–32	A15, A16	Wiped according to procedure	Unhappen
	33–36	A17, A18	Wiped according to procedure	Unhappen
	37–40, 41–44	A19–A22	Not wiped	Happened
	45–48	A23, A24	Wiped according to procedure	Unhappen
	49–52	A25, A26	Wiped according to procedure	Unhappen
	53–56	A27, A28	Not wiped	Happened
	57–60	A29, A30	Wiped according to procedure	Unhappen

non-metallic materials in the Phase II tests can be considered negligible, and there is no need to sample and analyze the channel or brush surface debris. After disassembling Product B for cover inspection, microscopy equipment was used to photograph the debris. The results showed that the debris was grayish-brown and flocculent, adhering to the brush filaments, as shown in Figure 11. The distinct difference in debris morphology (granular vs. flocculent) between Product A and Product B, despite identical friction pair materials, suggests that the presence of condensed volatiles on the friction interface of Product B may have acted as a binder or medium, causing the metallic wear particles to adhere and aggregate into flocculent structures.

Comparing the state of the wear debris indicates that the slip ring test product exhibits abnormal wear debris. Additionally, microscopic photographs were taken of the brush surface and the ring groove. The wear condition of the brush surface is shown in Figure 12, illustrating the brush surface states (a) and (b).

As shown in Figures 11 and 12, there is flocculent wear debris at the contact area of the ring brush. The debris adheres to the surface of the bristles, which exhibit obvious wear patterns, while the ring lane surface shows no evident wear. Preliminary analysis suggests that there may be some extraneous material on the friction pair surfaces causing the abnormal state of the wear debris. Due to abnormal results in low-current testing and monitoring under high vacuum and low-temperature conditions, the possibility of contamination of the product caused by the volatilization of non-metallic

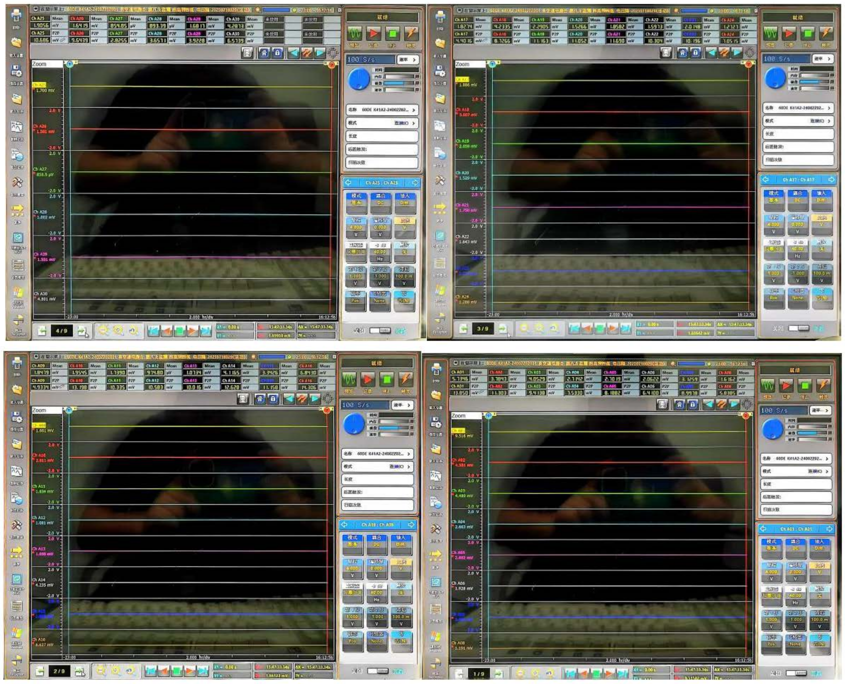

FIGURE 6. Monitoring curves of Product A under high and low temperature conditions in a vacuum environment

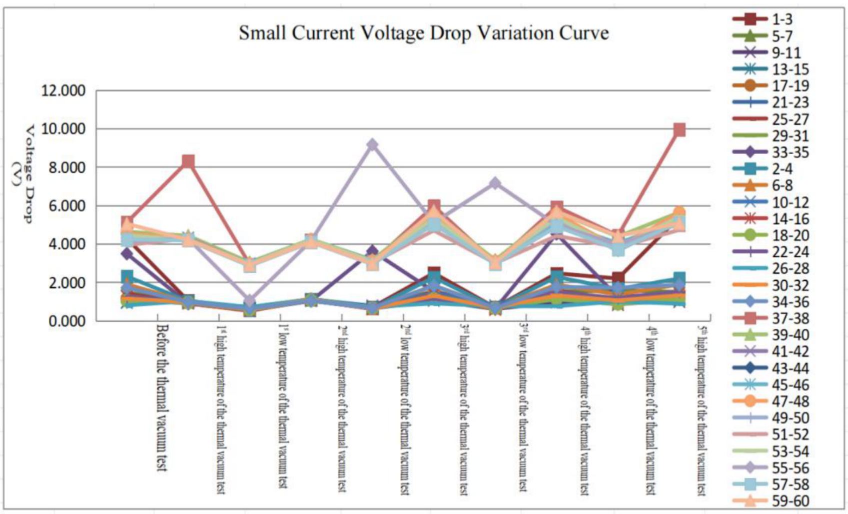

FIGURE 7. P2P Curve of Product B under Vacuum Environment High and Low Temperature Tests

materials in a vacuum environment cannot be ruled out.

Therefore, it is necessary to sample and analyze the wear debris on both the ring lane surface and the brush assembly. The results of the analysis of the machining swarf components are shown in Figure 13:

From the component analysis, it can be seen that the wear debris contains relatively high amounts of C, O, and Si elements, which can preliminarily be judged as organic matter[9].. However, it is not possible to determine which type of non-metallic material the organic matter originates from. Subsequently, spectral analysis was conducted on the non-metallic materials used in the development of the conductive slip ring. The non-metallic materials analyzed included polyimide, HY914, MS adhesive, GD-414C, E51 epoxy adhesive, and 3M tape. At the same time, a portion of the wear debris was sampled for spectral analysis. By comparing the results with the matching table provided below (Table 4), it was found that GD-414C showed a similarity of over 70.66 (a similarity exceeding 60 can be considered the same substance), indicating that the organic matter originates from GD-414C.

A. SPECTRAL ANALYSIS RESULTS

The results of the surface analysis of the test product's ring are shown in Figure 14. The spectral analysis of the test product after testing shows distinct peaks, indicating the

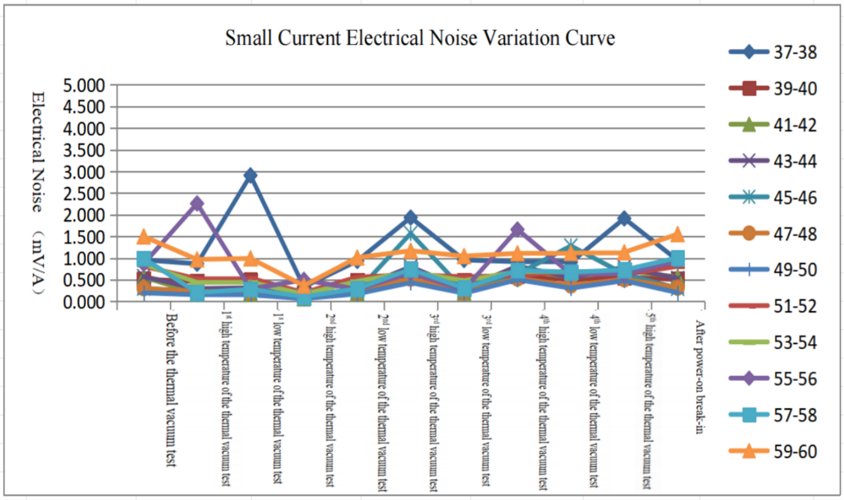

FIGURE 8. Electrical Noise Diagram of Product B under High and Low Temperature Tests in a Vacuum Environment

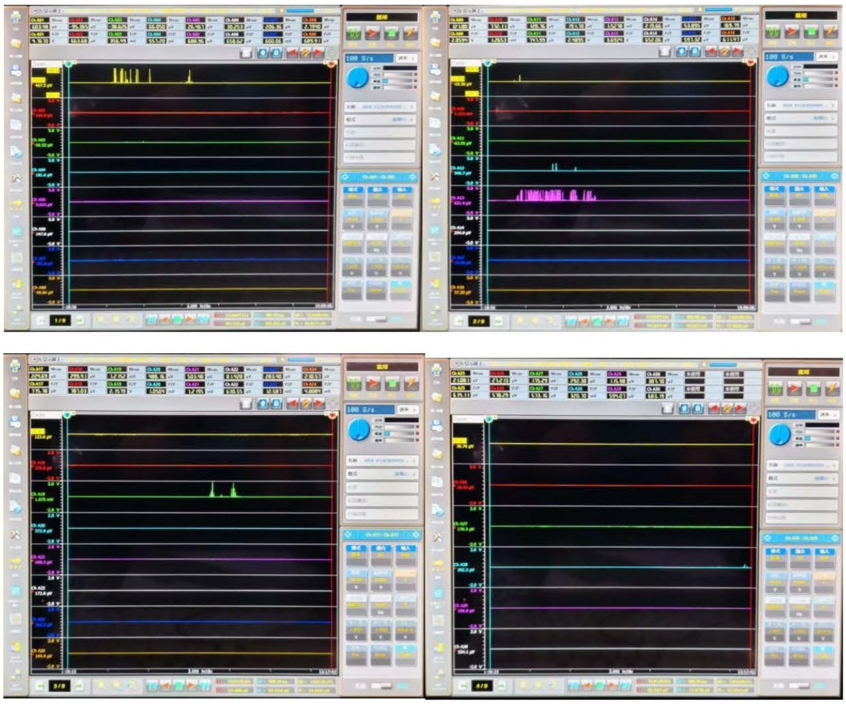

FIGURE 9. Monitoring Curve of Product B in High and Low Temperature Vacuum Environment

TABLE 4. Analysis Results Matching Table

S/N	Types of Organic Compounds	Similarity	Remark
	Talcum Powder 5519 Epoxy Adhesive	12.42	Standalone
	E51	22.34	Standalone
	GD-414C	70.66	Standalone
	HY914	13.85	Standalone
	KD504A	26.93	Standalone
	MS	23.21	Standalone
	Heat Shrink Tubing	12.00	Standalone
	Polyimide	5.81	Standalone
	3M Yellow Tape	31.90	Standalone

presence of organic substances. Spectral analysis was conducted on the organic materials used during the development of the slip ring product. Comparative analysis indicates that the organic material is GD-414C adhesive.

2) Product B of the slip ring test was disassembled, cleaned, wiped, and reassembled, followed by 4.5 cycles of vacuum power run-in. After the run-in, sampling and spectral analysis of debris on the surface of the slip ring were conducted. As shown in Figure 15, the spectral analysis of the wiped conductive slip ring did not show a significant presence of organic substances. After subjecting slip ring Product B to another vacuum volatilization contamination power test for non-metallic materials, the subsequent spectral analy-

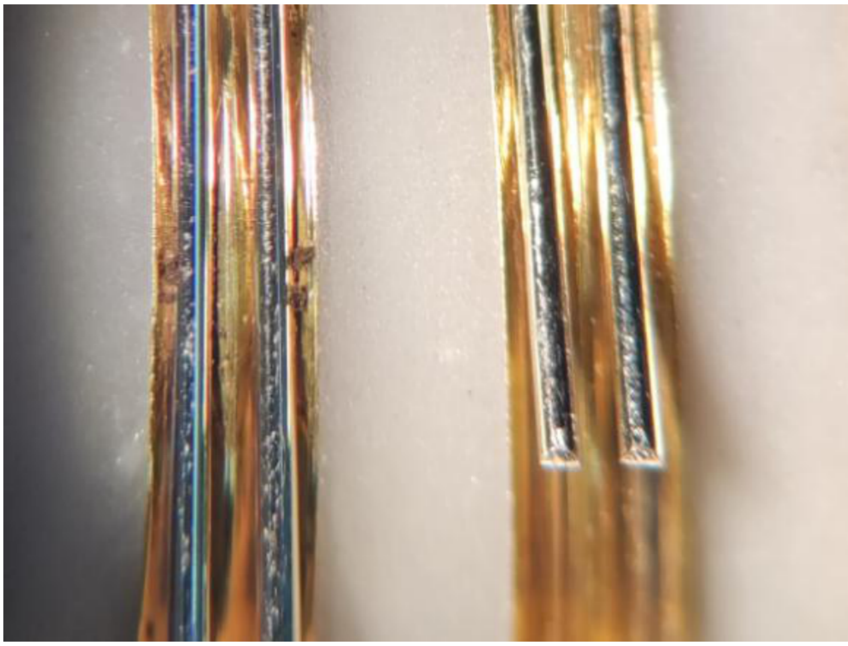

FIGURE 10. Status of Annular Wear Debris of Product A After High and Low Temperature Testing

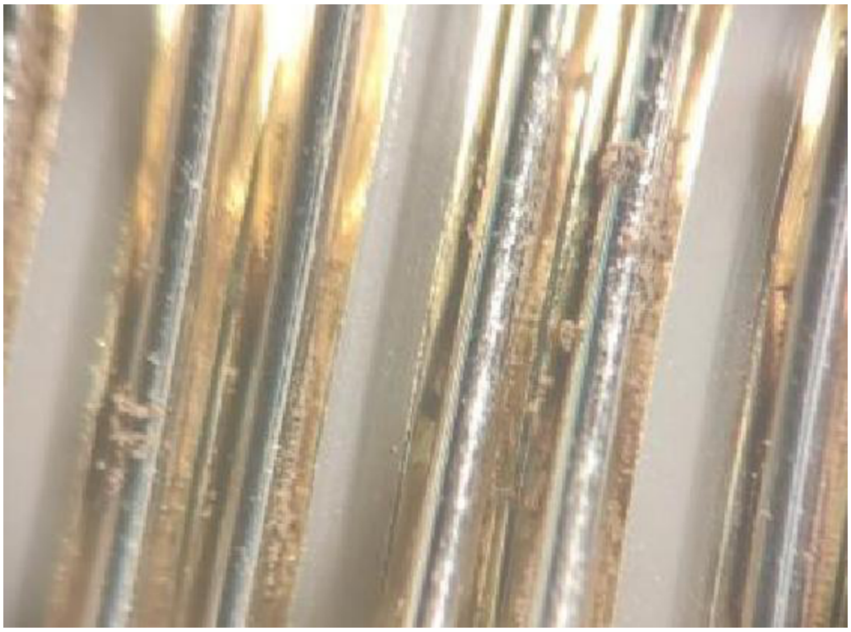

FIGURE 11. Status of Ring Channel Wear Debris of Product B After Vacuum Testing

sis indicated noticeable peaks, with their positions being generally consistent with the first test. Therefore, it can be concluded that GD-414C volatilized during the vacuum test and condensed on the contact surface of the conductive slip ring friction pair, causing electrical signal dynamic resistance anomalies.

The above experimental results indicate that the GD-414C adhesive undergoes vacuum volatilization and condensation on the contact surfaces of the friction pair, thereby causing an abnormal increase in the impedance of the conductive slip ring.

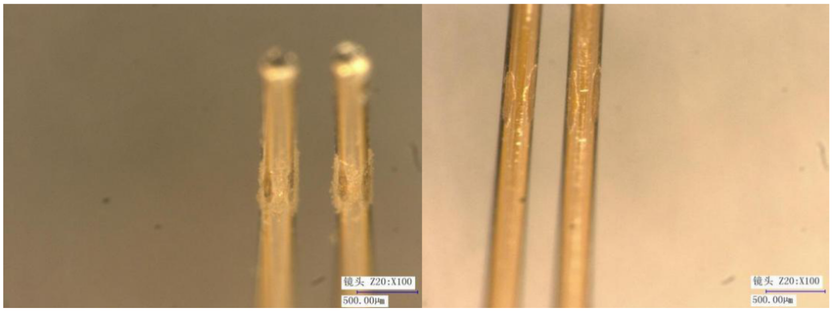

(a) (b)

FIGURE 12. Microscopic Images of Bristles and Annular Surface

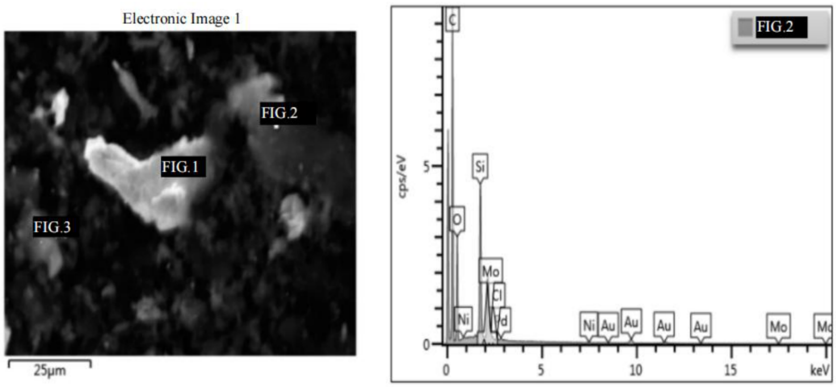

FIGURE 13. Analysis Results of Abrasive Debris Composition

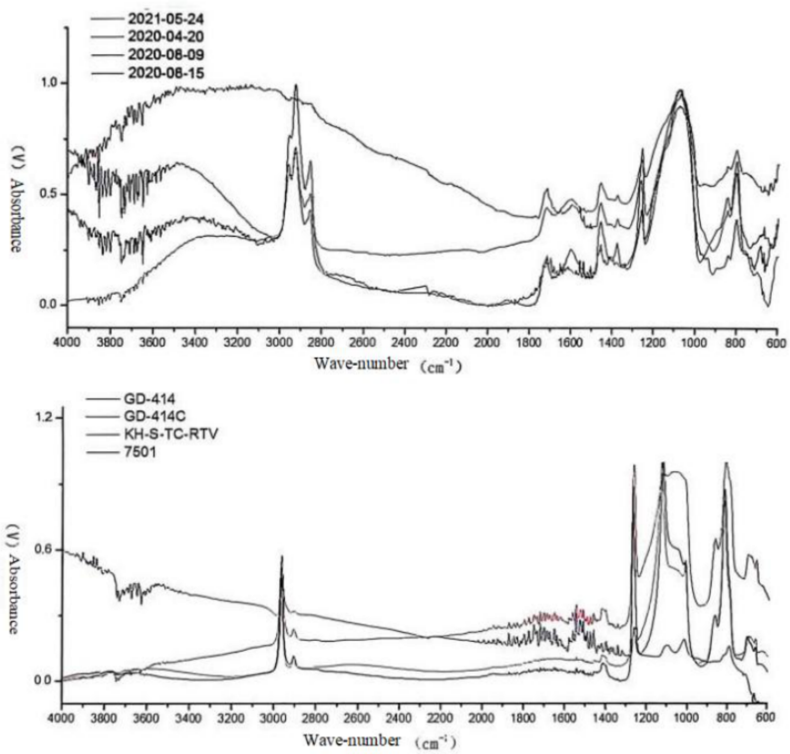

FIGURE 14. Spectral Analysis Results of the Conductive Slip Ring

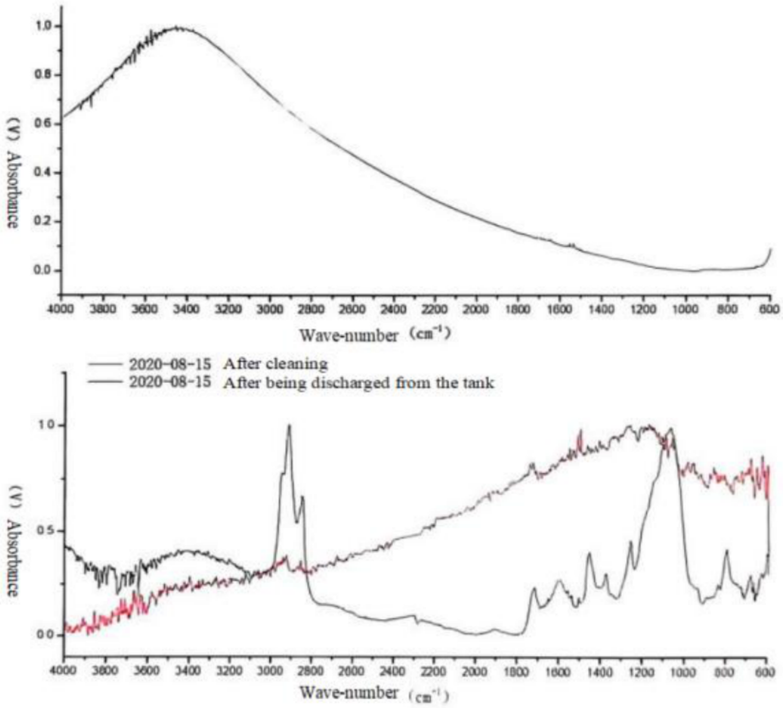

FIGURE 15. Spectral Analysis Results Before and After the Experiment

VI. CONCLUSION

(1) The condensation of organic volatiles on slip ring friction pairs in vacuum environments facilitates wear debris aggregation, leading to significant dynamic resistance fluctuations.

(2) After the conductive slip ring is contaminated by vacuum volatiles from non-metallic materials, the spectral analysis of sampled fibrous wear debris indicates that GD-414C adhesive, used during the development of the conductive slip ring, is the primary non-metallic material responsible for the electrical signal dynamic resistance anomalies of the product[10][11]..

(3) During the development of the conductive slip ring, to effectively prevent the impact of vacuum volatiles from non-metallic materials, the use of GD-414C adhesive should be controlled, and the product should undergo pre-vacuum degassing treatments. This ensures that electrical signal anomalies caused by vacuum outgassing of non-metallic materials during ground testing are eliminated.

AUTHOR CONTRIBUTIONS

Conceptualization –Zemin Hu, Yijian Wang, Bin Lv, Peng Luo, Hongming Ni, Fei Gao and Zengwei Zhou; methodology – Zemin Hu, Yijian Wang, Peng Luo, Hongming Ni, Fei Gao and Zengwei Zhou; investigation – Zemin Hu, Yijian Wang, Bin Lv, Peng Luo, Hongming Ni, Fei Gao and Zengwei Zhou; writing-original draft preparation – Zemin Hu, Yijian Wang, Bin Lv, Peng Luo, Hongming Ni, Fei Gao and Zengwei Zhou. All authors have read and agreed to the published version of the manuscript.

CONFLICTS OF INTEREST

The authors declare no conflict of interest.

FUNDING

This work was supported by Jiangxi Province "Ganpo Juncai" Support Program-Leading Academic and Technological Leaders in Key Disciplines. (Project Number: 20243BCE51183).

ACKNOWLEDGEMENTS

Not applicable.

REFERENCES

[1] M. Antler, “Electrical effects of fretting connector contact materials: A review,” Wear, vol. 106, no. 1-3, pp. 5-33, 1985, doi: 10.1016/0043-1648(85)90101-2.
[2] X. Luo, P. Li, Q. Zhou, J. Chen, Q. Zhang, Y. Liu, et al., “Investigation on Friction and Wear Behavior of Space Conductive Slip Rings under Vacuum Current-carrying Conditions,” Equipment Environmental Engineering, vol. 22, no. 6, pp. 55-65, 2025, doi: 10.7643/issn.1672-9242.2025.06.007.
[3] J. Wang, S. Zhang, T. Zhang, J. Liu, G. Zhou, J. Zhang, et al., “Reconstruction of wear debris migration trajectory and analysis of motion characteristics in on-orbit spacecraft conductive slip rings,” Space Solar Power and Wireless Transmission, vol. 2, no. 2, pp. 81-90, 2025, doi: 10.1016/j.sspwt.2025.06.002.
[4] N. Argibay, J. A. Bares, and W. G. Sawyer, “Asymmetric wear behavior of self-mated copper fiber brush and slip-ring sliding electrical contacts in a humid carbon dioxide environment,” Wear, vol. 268, no. 3-4, pp. 455-463, 2010, doi: 10.1016/j.wear.2009.08.036.
[5] M. Grandin and U. Wiklund, “Influence of mechanical and electrical load on a copper/copper-graphite sliding electrical contact,” Tribology International, vol. 121, pp. 1-9, 2018, doi: 10.1016/j.triboint.2018.01.004.
[6] A. Bouchoucha, S. Chekroud, and D. Paulmier, “Influence of the electrical sliding speed on friction and wear processes in an electrical contact

copper–stainless steel," Applied surface science, vol. 223, no. 4, pp. 330-342, 2004, doi: 10.1016/j.apsusc.2003.09.018.

[7] A. C. Tribble, B. Boyadjian, J. Davis, J. Haffner, and E. McCullough, "Contamination control engineering design guidelines for the aerospace community," in Optical System Contamination V, and Stray Light and System Optimization, vol. 2864, pp. 4-15, SPIE, 1996, doi: 10.1117/12.258298.

[8] L. Niu, H. You, H. Lv, Y. Jiang, G. Zhou, C. Li, et al., "Influence of vacuum baking O-rings on optical properties of laser system," High Power Laser and Particle Beams, vol. 35, no. 6, pp. 061004-1, 2023, doi: 10.11884/HPLPB202335.220390.

[9] A. Banerjee, J. G. Zhang, M. Garshasb, L. R. Zhang, and R. W. Vook, "Wear debris analysis in rotating Ag-Cu electrical contacts," Wear, vol. 84, no. 1, pp. 97-109, 1983, doi: 10.1016/0043-1648(83)90122-9.

[10] B. Singh, J. G. Zhang, B. H. Hwang, and R. W. Vook, "Microstructural characterization of rotating Cu-Cu electrical contacts in vacuum and wet CO2 environments," Wear, vol. 78, no. 1-2, pp. 17-28, 1982, doi: 10.1016/0043-1648(82)90015-1.

[11] J. C. Chen and R. Vook, "Characterization of sliding Al-Cu electrical contacts," IEEE transactions on components, hybrids, and manufacturing technology, vol. 9, no. 1, pp. 17-22, 1986, doi: 10.1109/TCHMT.1986.1136626.